ISSN 0208-7774 TRIBOLOGIA 4/2020 p. 59–70
DOI: 10.5604/01.3001.0014.5908

Andrzej RYNIEWICZ[*], Anna M. RYNIEWICZ[**], Łukasz BOJKO[***], Paweł PAŁKA[****], Wojciech RYNIEWICZ[*****]

THE ASSESSMENT OF THE LAYERED STRUCTURE OF PROSTHETIC CROWNS IN MICROSCOPIC EXAMINATIONS

OCENA WARSTWOWEJ BUDOWY KORON PROTETYCZNYCH W BADANIACH MIKROSKOPOWYCH

Key words: veneering layers, digital frameworks, EDS, adhesion.

Abstract: Prosthetic crowns are made in accordance with the principles of clinical procedures while taking into account the rules of endurance, biocompatibility, and aesthetics. Depending on the biomaterial and manufacturing technology, crown frameworks are veneered with an appropriate set of ceramics with selected thermal expansion. The veneering layers responsible for tribological cooperation in occlusal contact should properly adhere to the framework. The aim of the research is to conduct the microscopic and EDS chemical analysis to evaluate the process of shaping veneering layers on frameworks produced using new digital technologies, i.e. the technology of milling and laser sintering. The research material consists of specimens produced in perpendicular cross-sections through the layered structures of metal-ceramic, ceramic-veneered glass-ceramic, and zirconium crowns. The microscopic examinations were carried out using the specimens and included the elemental EDS analysis performed on the surfaces and in certain points. The structures of metal and ceramic frameworks, ceramic veneering layers, and adhesive zones were determined.

Słowa kluczowe: warstwy licujące, podbudowy cyfrowe, EDS, adhezja.

Streszczenie: Korony protetyczne wykonywane są zgodnie z procedurami klinicznymi oraz ze wskazaniami wytrzymałości, biozgodności i estetyki. Podbudowy koron, w zależności od zastosowanego biomateriału i technologii wytworzenia, poddawane są licowaniu odpowiednim zestawem ceramik o dobranej ekspansji termicznej. Warstwy licujące, odpowiedzialne za współpracę tribologiczną w kontakcie okluzyjnym, powinny charakteryzować się właściwą adhezją do podbudowy. Celem przeprowadzonych badań jest analiza mikroskopowa i chemiczna EDS pozwalająca ocenić proces kształtowania warstw licujących na podbudowach wytworzonych w nowych technologiach cyfrowych: w technologii frezowania oraz w technologii spiekania laserowego. Materiałem badań są zgłady wykonane w przekrojach prostopadłych przez warstwowe struktury koron: metalowo-ceramicznych, szklano-ceramicznych licowanych ceramiką i cyrkonowych licowanych ceramiką. Na zgładach przeprowadzono badania mikroskopowe z analizą pierwiastkową EDS na powierzchniach oraz w punktach. Identyfikowano struktury metalowych i ceramicznych podbudów oraz strukturę ceramicznych warstw licujących wraz ze strefami adhezyjnymi.

[*] ORCID: 0000-0003-3437-7650. State University of Applied Sciences, Institute of Technology, ul. Zamenhofa 1a, 33-300 Nowy Sącz, Poland.

[**] ORCID: 0000-0003-2469-6527. Jagiellonian University Medical College, Faculty of Medicine, Dental Institute, Department of Dental Prosthodontics, ul. Montelupich 4, 31-155 Cracow, Poland.

[***] ORCID: 0000-0002-6024-458X. AGH University of Science and Technology, Faculty of Mechanical Engineering and Robotics, al. Mickiewicza 30, 30-059 Cracow, Poland.

[****] ORCID: 0000-0003-0640-7939. AGH University of Science and Technology, Faculty of Non-Ferrous Metals, al. Mickiewicza 30, 30-059 Cracow, Poland.

[*****] ORCID: 0000-0002-9140-198X. Jagiellonian University Medical College, Faculty of Medicine, Dental Institute, Department of Dental Prosthodontics, ul. Montelupich 4, 31-155 Cracow, Poland.

INTRODUCTION

Prosthetic crowns are made in accordance with the principles of clinical procedures while taking into account the rules of endurance, biocompatibility, and aesthetics. Depending on the biomaterial and manufacturing technology, crown frameworks are veneered with an appropriate set of ceramics. Ceramics are inorganic and non-metallic biomaterials that are processed by high-temperature firing. The veneering layers of the framework are responsible for the functional and biomechanical cooperation with the opposing teeth. They should ensure adhesion of successively applied opaque, dentin and enamel layers and proper adhesion to the load-bearing framework. The topic is important because new biomaterials are used in modern prosthetics as well as the CAD/CAM system for designing and production of load-bearing structures, and this creates a need to assess the quality of veneering layers.

The aim of the research is to conduct the microscopic and EDS chemical analysis to evaluate the process of shaping veneering layers on frameworks produced using new digital technologies, i.e. the technology of milling from matrices and laser sintering from selective metal powders.

MATERIAL AND METHOD

The research material consists of specimens produced in perpendicular cross-sections through the layered structures of prosthetic crowns, namely, through the ceramic veneering layers and load-bearing layers. The following structures were tested: chromium-cobalt veneered with Duceram Kiss ceramics, pure titanium and Ti6Al4V alloyed titanium frameworks veneered with Vita Titankeramik ceramics, glass-ceramic frameworks veneered with IPS e.max Ceram, and zirconium frameworks veneered with Elephant Sakura ceramics. The test sample kits were made in professional laboratories in accordance with the latest knowledge of the innovative technology for producing fixed prosthetic restorations. The samples of materials for load-bearing frameworks in the form of ø1/4" discs with a thickness of 1/16", 9 pieces each, were made of factory matrices from CoCrMo alloy, TiCP titanium, Ti6Al4V alloy, $Li_2Si_2O_5$ ceramics, and ZrO_2 ceramics, using the technology of milling in the CAD/CAM system using the CORiTEC 350i by imes icore. The ZrO_2 discs were milled adequately larger (expansion coefficient 24%), so that, after sintering, they achieved the proper structure and the desired dimensions. The same discs made of materials for load-bearing frameworks using the Selective Laser Melting (SLM) method in the CAD/CAM system, 9 pieces each, were sintered from CoCrMo powders and Ti6Al4V powders using a Renishaw AM250 machine. The discs prepared in this way, which were produced using the milling technology and the incremental sintering technology, were subjected to the processes of preparing the superficial layer of the framework and the application of successive layers of dedicated ceramics and firing of the layers (**Fig. 1**). The preparation of the specimens consisted of sinking the discs in resin. After the resin condensation process, the discs were mounted in a special holder and cut with a diamond disc in a water bath. The next stage of sample preparation was multi-stage polishing using an automatic polisher by Struers and degreasing the surface of the specimens (**Fig. 2**).

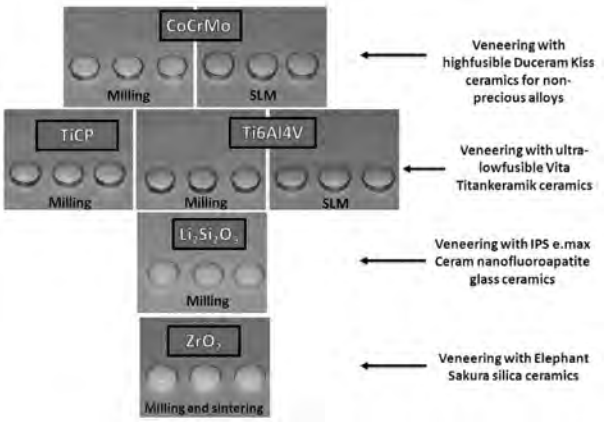

Fig. 1. Test discs with a layered veneering structure dedicated to prosthetic frameworks made using the CAD/CAM milling technology and SLM technology [L. 1]

Rys. 1. Krążki badawcze z wytworzoną warstwową strukturą licującą dedykowaną podbudowom protetycznym z technologii frezowania CAD/CAM oraz z technologii SLM **[L. 1]**

Fig. 2. Specimens for the analysis of layered structures of prosthetic crowns

Rys. 2. Zgłady do analiz struktur warstwowych koron protetycznych

The analysis of microstructure and chemical composition measurements were performed for the specimens using Hitachi S-3400N SEM scanning microscopy, equipped with a Thermo Noran X-ray dispersion energy spectrometry EDS attachment. The tests were carried out at an accelerating voltage of 20 kV, using the low vacuum technique. A pressure of 30 Pa was used. This allowed for electron microscopic observations in the contrast of BSE (backscattered electron) as well as for the measurements of chemical composition.

RESULTS AND DISCUSSION

The SEM image of the Duceram Kiss – CoCrMo composition obtained using the milling technology is characterized by a homogeneous framework with large equiaxial grains and very small precipitates (**Fig. 3**). Very small and few pores are visible. Points 1 and 2 of the framework contain Co, Cr, Mo, W, and small amounts of Al, Si, and K (**Tab. 1**). Points 3–6 contain the opaque and opaque dentin which connects the framework to the dentin. The connection is the result of chemisorption through diffusion between the surface of the oxides on the alloy and the ceramics. These oxides are formed when the alloy is wetted with ceramics and during firing of ceramics. The points contain over 40 wt.% O and Na, Al, Si, K, and Point 6 – Sn. Such a chemical composition and weight proportions indicate the presence of $KAlSi_2O_6$ and Na_2O oxides in the opaque and opaque dentin. Numerous spherical-shaped gas pores are visible in this zone. The opaque oxide layer forms another adhesive bond with the dentin layer, which in addition to oxides based on Na, Al, Si and Ca, is rich in Y and ZrO_2 (Points 8 and 9).

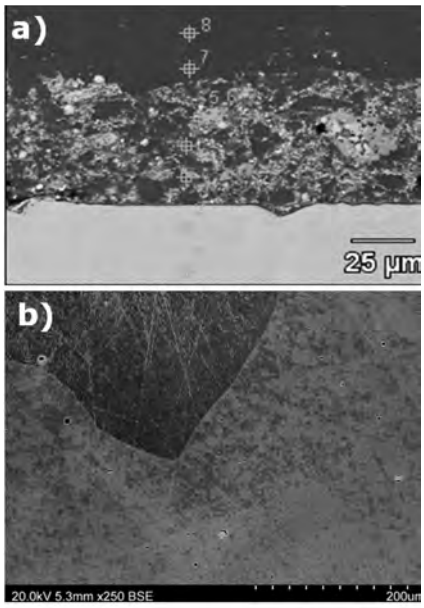

Fig. 3. The SEM image of the microstructure of the Duceram Kiss-CoCrMo material composition made using the milling technology: a) with points marked for the analysis of the chemical composition, b) image for the analysis of the structure of the framework

Rys. 3. Obraz SEM mikrostruktury kompozycji materiałowej Duceram Kiss – CoCrMo z technologii frezowania: a) z zaznaczonymi punktami do analizy składu chemicznego, b) obraz do analizy struktury podbudowy

Figure 4 shows the undesirable mechanical damage to the Duceram Kiss – CoCrMo layered material composition made using the milling technology. This may be the case with some alloys forming Cr_2O_2-rich

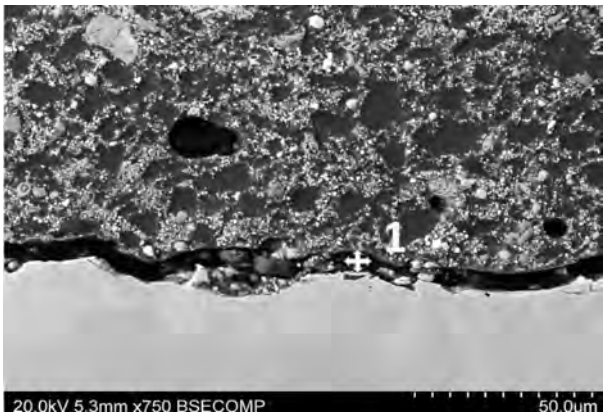

Fig. 4. Damage to the interface of the Duceram Kiss – CoCrMo border made using the milling technology

Rys. 4. Uszkodzenie w interfazie strefy granicznej Duceram Kiss – CoCrMo z technologii frezowania

oxide layers that do not adhere well to the alloy **[L. 2]**. The reason for this may be the lack of the application of a binding agent that modifies the oxide layer. This structure was described in Point 1 with 18.25 wt.% Cr and 18.66 wt.% O. The interface of the veneering-framework border may be damaged when the oxides do not completely melt during firing of the opaque.

The SEM image of the Duceram Kiss-CoCrMo composition obtained using laser sintering is characterized by a framework made of equiaxial grains and grains with a highly elongated shape (**Fig. 5**). At the grain boundaries, there are few porosities. Apart from Co, Cr, Mo, Points 1 and 2 in the framework zone contain small amounts of Al and K, and slightly more Si (**Tab. 2**). There is a thin opaque transition layer on the framework which creates a uniform interface without voids. Co is also present in the 1 µm thick transition layer, slightly less Cr than in the framework, Mo and W – approx. 5.5 wt.%. Moreover, there are Al, Si, and K (Point 3).

The opaque layer is made of oxides. This is evidenced by the high content of O – 43.39 wt.%, Al, Si, Zr, K and Na (Point 4). It also contains small amounts of Co and Cr (Point 4). The amount of oxides in the opaque is confirmed by the stoichiometric content of oxygen, metals, and non-metals (Points 5 and 6). The elements present are Si, Al, In, Na, Cr, Zr, and a small amount of P. The opaque layer contains numerous spherical pores. Dentin is also a mixture of oxides (items 7 and 8). The presence of oxides is indicated by the contents of 45.74 wt.% – O and Si, K, Al and lower contents of Na and Zr.

The TiCP and Ti6Al4V discs from milling and the Ti6Al4V discs from incremental sintering were veneered with low-melting point Vita Titankeramik ceramics. In the SEM image of the microstructure of Vita Titankeramik – TiCP, the framework is homogeneous with a tightly packed crystal network built of β phase. Points 1 and 2 show the content of titanium in about

Table 1. Chemical composition of the selected points on the specimen surface in a sample of CoCrMo alloy made using the milling technology veneered with Duceram Kiss ceramics

Tabela 1. Skład chemiczny w wybranych punktach na powierzchni zgładu w próbce ze stopu CoCrMo z technologii frezowania licowanej ceramiką Duceram Kiss

Point	Concentration (wt.%)												
	Element												
	O	Na	Al	Si	K	Ca	Cr	Co	Y	Zr	Mo	Sn	W
1	–	–	0.74	1.26	0.32	–	25.65	58.56	–	–	3.00	–	10.46
2	–	–	0.82	1.28	0.45	–	26.85	57.69	–	–	3.48	–	8.50
3	42.66	2.53	9.13	28.87	10.39	–	2.25	4.17	–	–	–	–	–
4	41.01	1.66	10.95	26.68	11.30	–	2.58	5.82	–	–	–	–	–
5	40.00	3.46	5.77	21.73	8.15	–	2.52	3.88	–	–	–	14.49	–
6	45.19	4.27	6.73	31.98	7.59	–	1.64	2.60	–	–	–	–	–
7	46.23	4.33	6.90	30.98	7.62	–	1.14	2.81	–	–	–	–	–
8	37.16	2.36	2.37	15.40	3.45	0.31	1.52	3.32	34.10	–	–	–	–
9	30.35	–	0.55	3.44	0.83	–	1.37	3.20	–	60.26	–	–	–
	Atomic (%)												
Point	Element												
	O	Na	Al.	Si	K	Ca	Cr	Co	Y	Zr	Mo	Sn	W
1	–	–	1.79	2,81	0.74	–	29.20	58.54	–	–	2.38	–	4.54
2	–	–	2.01	2.88	1.04	–	30.07	56.59	–	–	2.96	–	4.45
3	56.31	3.04	8.82	22.87	6.12	–	1.08	1.76	–	–	–	–	–
4	57.88	1.63	9.17	21.45	6.52	–	1.12	2.23	–	–	–	–	–
5	61.24	3.68	5.24	18.95	5.10	–	1.19	1.61	–	–	–	2.99	–
6	60.51	3.98	5.34	24.39	4.16	–	0.68	0.95	–	–	–	–	–
7	61.47	4.00	5.44	23.46	4.15	–	0.47	1.01	–	–	–	–	–
8	64.05	2.83	2.42	15.12	2.43	0.21	0.81	1.55	10.58	–	–	–	–
9	67.69	–	0.73	4.37	0.76	–	0.94	1.94	–	23.57	–	–	–

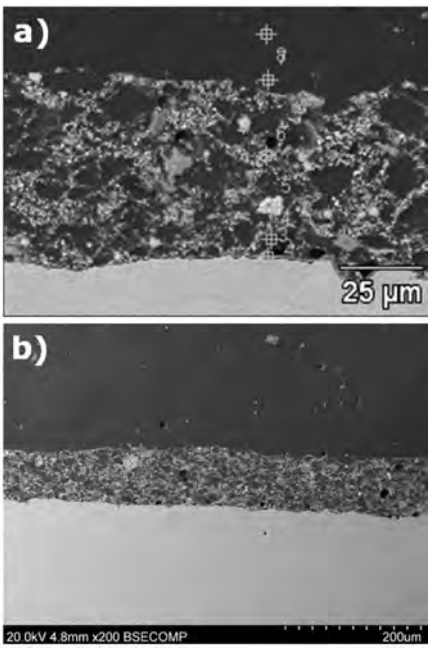

Fig. 5. The SEM image of the microstructure of the Duceram Kiss – CoCrMo material composition made using the SLM technology: a) with points marked for the chemical composition analysis, b) the SEM image for structure analysis

Rys. 5. Obraz SEM mikrostruktury kompozycji materiałowej Duceram Kiss – CoCrMo z technologii SLM: a) z zaznaczonymi punktami do analizy składu chemicznego, b) obraz SEM do analizy struktury

99 wt.% (**Fig. 6, Tab. 3**). In addition, there are small amounts of Si, Al, and K that may come from the preparation of titanium surfaces for bonding to ceramics. The process of surface preparation consisted of jet cleaning, etching, and the use of intermediate layers **[L. 1]**. In order to ensure a better contact of the titanium biomaterial with the ceramics, an intermediate layer – bonder was used. Point 3 is representative for the chemical composition of this layer. A large proportion of oxygen is typical, as are the elements that form the oxides: Si, Na, K, Ti, Al, Ca, and Mg. In about 90 µm thick layer of the bonder, numerous large and smaller pores are visible.

The pores are the result of air being trapped during the sintering process. Under the influence of surface tension, air spaces become spherical and expand with an increase of the temperature. The zones with a diffusion effect are visible at the connection between the bonder and the framework. The bonder provides a 25 µm thick connection to the opaque (Points 4 and 5). This layer is composed of the following oxides: SiO_2, Al_2O_3, K_2O, Na_2O, TiO_2, ZrO_2. This is the crystalline phase contained in the glass matrix. The opaque layer contains a large number of spherical pores. Points 6 and 7 are representative of dentin. Its structure is uniform – melted down, with small pores. This layer is also composed of oxides. The high content of SiO_2 and ZrO_2 is similar to opaque, but with less Al_2O_3, K_2O, Na_2O, TiO_2, also CaO.

The SEM image of the Vita Titankeramik-Ti6Al4V microstructure obtained using the milling technology

Table 2. Chemical composition of the selected points on the specimen surface in a sample of CoCrMo alloy made using the SLM technology veneered with Duceram Kiss ceramics

Tabela 2. Skład chemiczny w wybranych punktach na powierzchni zgładu w próbce ze stopu CoCrMo z technologii SLM licowanej ceramiką Duceram Kiss

Concentration (wt.%)												
Point	Element											
	O	Na	Al	Si	P	K	Cr	Co	Zr	Mo	In	W
1	–	–	0.95	5.39	–	0.34	25.17	62.45	–	5.70	–	–
2	–	–	0.91	6.19	–	0.57	24.44	62.06	–	5.83	–	–
3	–	–	1.21	3.54	–	0.85	19.97	64.65	–	4.29	–	5.49
4	43.39	0.69	38.50	4.39	–	1.51	2.07	5.38	4.07	–	–	–
5	45.82	1.65	6.72	23.52	1.29	9.85	1.95	4.98	–	–	4.22	–
6	47.93	3.36	6.23	24.82	–	0.00	2.39	5.87	3.25	–	6.14	–
7	43.69	2.59	7.86	26.36	–	10.60	1.36	2.43	5.11	–	–	–
8	45.74	4.07	7.28	30.54	–	9.01	1.19	2.18	–	–	–	–
Atomic (%)												
Point	Element											
	O	Na	Al	Si	P	K	Cr	Co	Zr	Mo	In	W
1	–	–	1.91	10.43	–	0.48	26.33	57.62	–	3.23	–	–
2	–	–	1.82	11.90	–	0.78	25.37	56.84	–	3.28	–	–
3	–	–	2.57	7.22	–	1.24	21.96	62.75	–	2.56	–	1.71
4	59.74	0.66	31.43	3.44	–	0.85	0.88	2.01	0.98	–	–	–
5	64.00	1.60	5.57	18.72	0.93	5.63	0.84	1.89	–	–	0.82	–
6	66.70	3.26	5.14	19.68	–	0.00	1.02	2.22	0.79	–	1.19	–
7	61.12	2.52	6.52	21.01	–	6.07	0.58	0.92	1.25	–	–	–
8	61.04	3.78	5.76	23.22	–	4.92	0.49	0.79	–	–	–	–

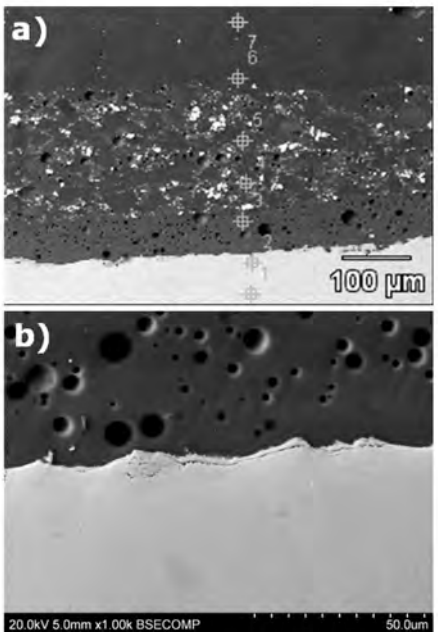

Fig. 6. The SEM image of the microstructure of the Vita Titankeramik – TiCP material composition made using the milling technology: a) with points marked for the analysis of the chemical composition, b) the area of the framework – bonder with the areas of diffusion

Rys. 6. Obraz SEM mikrostruktury kompozycji materiałowej Vita Titankeramik – TiCP z technologii frezowania: a) z zaznaczonymi punktami do analizy składu chemicznego, b) strefa podbudowa – bonder z obszarami dyfuzji

is different in the subsequent layers. The framework is characterized by a granular and homogeneous microstructure (Point 1). The grains are regular in shape. Precipitations are visible at the grain boundary. The contents of the elements Ti, Al, V correspond to the stoichiometric composition of the Ti6Al4V compound. The wt.% composition of Point 1 shows a small amount of Si – probably coming from the sandblasting process. Point 2 is located in a 2–3 µm thick bonder. The following oxides can be identified as the interphase: SiO_2, Al_2O_3, TiO_2, Na_2O, K_2O, TiO_2, CaO, and MgO. Diffusion effects are visible between the opaque and bonder. The next layer, 250 µm thick, is an opaque. It is made of the following oxides: SiO_2, Al_2O_3, K_2O, Na_2O, TiO_2, and CaO. Points 3–5 are representative (**Fig. 7, Tab. 4**). ZnO is present in Point 4. The content of Al_2O_3 decreases as it approaches the dentin layer. There are numerous spherical pores in the opaque layer. The chemical composition of Point 6 is representative of dentine. Its structure is homogeneous. When melted down, there is the highest content of SiO_2 oxides in the structure. In addition, there are the following oxides: K_2O, Na_2O, Al_2O_3, TiO_2, and CaO.

The same set of Vita Titankeramik ceramics was used to veneer the framework made of the Ti6Al4V alloy, but using the SLM technology (**Fig. 8, Tab. 5**). The framework consists of Ti, Al, and V (Points 1 and 2). It has a homogeneous two-phase structure of the needle-shaped-lamellar nature, consisting of the β phase and the α-phase precipitates with the shape of

Table 3. Chemical composition of the selected points on the specimen surface in a pure titanium TiCP sample made using the milling technology veneered with the Vita Titankeramik ceramics

Tabela 3. Skład chemiczny w wybranych punktach na powierzchni zgładu w próbce z czystego tytanu TiCP z technologii frezowania licowanej ceramiką Vita Titankeramik

Concentration (wt.%)									
Point	Element								
	O	Na	Mg	Al	Si	K	Ca	Ti	Zr
1	–	–	–	–	1.10	–	–	98.90	–
2	–	–	–	0.27	1.88	0.29	–	97.57	–
3	54.57	3.43	0.47	2.92	27.66	3.21	2.27	5.47	–
4	50.95	5.87	–	7.57	24.75	5.88	–	4.99	–
5	48.97	2.74	–	8.44	25.38	10.85	–	2.93	0.67
6	50.60	3.86	–	2.93	26.49	5.14	1.09	2.21	7.68
7	53.65	4.04	–	2.35	31.74	5.58	1.41	1.24	–
Atomic (%)									
Point	Element								
	O	Na	Mg	Al	Si	K	Ca	Ti	Zr
1	–	–	–	–	1.86	–	–	98.14	–
2	–	–	–	0.47	3.15	0.34	–	96.03	–
3	69.25	3.03	0.40	2.20	19.99	1.67	1.15	2.32	–
4	65.58	5.26	–	5.77	18.15	3.10	–	2.14	–
5	64.54	2.51	–	6.60	19.06	5.85	–	1.29	0.15
6	67.70	3.59	–	2.32	20.19	2.82	0.58	0.99	1.80
7	67.75	3.55	–	1.76	22.83	2.88	0.71	0.52	–

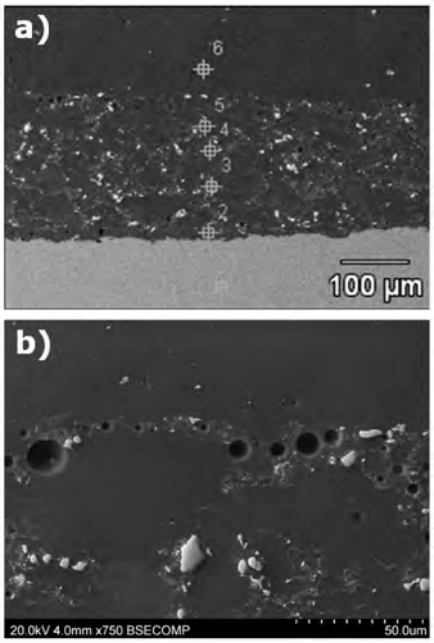

Fig. 7. The SEM image of the microstructure of the Vita Titankeramik – Ti6Al4V material composition made using the milling technology: a) with points marked for the analysis of the chemical composition, b) the border of the opaque – dentine

Rys. 7. Obraz SEM mikrostruktury kompozycji materiałowej Vita Titankeramik – Ti6Al4V z technologii frezowania: a) z zaznaczonymi punktami do analizy składu chemicznego, b) granica opaker – dentyna

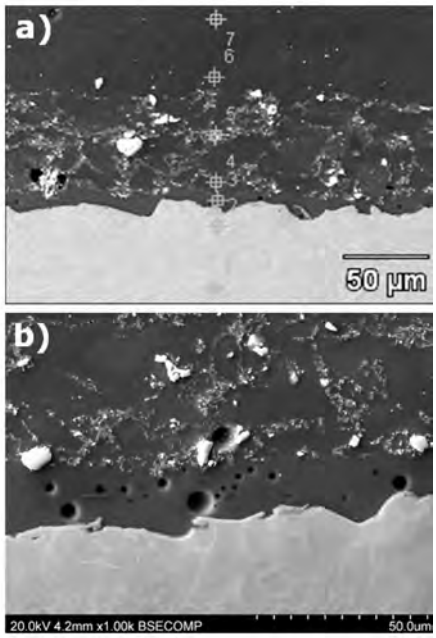

Fig. 8. The SEM image of the microstructure of the Vita Titankeramik – Ti6Al4V material composition made using the SLM technology: a) with points marked for chemical composition analysis, b) magnification 1000x

Rys. 8. Obraz SEM mikrostruktury kompozycji materiałowej Vita Titankeramik – Ti6Al4V z technologii SLM: a) z zaznaczonymi punktami do analizy składu chemicznego, b) powiększenie 1000x

Table 4. Chemical composition of the selected points on the specimen surface in a sample of Ti6Al4V alloy made using the milling technology veneered with Vita Titankeramik ceramics

Tabela 4. Skład chemiczny w wybranych punktach na powierzchni zgładu w próbce ze stopu Ti6Al4V z technologii frezowania licowanej ceramiką Vita Titankeramik

Concentration (wt.%)										
Point	Element									
	O	Na	Mg	Al	Si	K	Ca	Ti	V	Zn
1	–	–	–	5.84	1.08	–	–	89.61	3.47	–
2	54.73	4.32	0.48	3.40	24.84	3.40	2.19	6.63	–	–
3	50.77	4.59	–	6.36	24.65	6.56	–	7.08	–	–
4	51.84	5.49	–	3.57	28.27	4.76	0.93	4.63	–	0.50
5	53.96	4.80	–	2.93	30.02	4.65	1.23	2.42	–	–
6	53.50	4.41	–	2.41	31.38	5.45	1.25	1.61	–	–
Atomic (%)										
Point	Element									
	O	Na	Mg	Al	Si	K	Ca	Ti	V	Zn
1	–	–	–	9.86	1.75	–	–	85.28	3.10	–
2	69.54	3.82	0.40	2.56	17.98	1.77	1.11	2.81	–	–
3	66.09	4.16	–	4.91	18.28	3.49	–	3.08	–	–
4	66.57	4.91	–	2.72	20.68	2.50	0.48	1.98	–	0.16
5	68.01	4.21	–	2.19	21.55	2.40	0.62	1.02	–	–
6	67.60	3.88	–	1.81	22.59	2.82	0.63	0.68	–	–

Table 5. Chemical composition of the selected points on the specimen surface in a sample of Ti6Al4V alloy made using the SLM technology veneered with Vita Titankeramik ceramics

Tabela 5. Skład chemiczny w wybranych punktach na powierzchni zgładu w próbce ze stopu Ti6Al4V z technologii SLM licowanej ceramiką Vita Titankeramik

Concentration (wt.%)										
Point	Element									
	O	Na	Mg	Al	Si	K	Ca	Ti	V	Zr
1	–	–	–	6.68	1.41	–	–	89.35	2.56	–
2	–	–	–	7.05	1.99	–	–	88.55	2.41	–
3	53.64	3.65	0.41	3.17	26.79	3.88	1.71	6.75	–	–
4	51.32	4.26	–	7.71	24.40	6.43	–	5.88	–	–
5	50.88	3.74	–	3.07	16.19	2.83	1.37	19.49	–	2.43
6	53.77	4.03	–	2.58	29.77	5.18	1.38	3.30	–	–
7	54.13	3.06	–	1.86	32.97	4.33	1.10	2.56	–	–
Atomic (%)										
Point	Element									
	O	Na	Mg	Al	Si	K	Ca	Ti	V	Zr
1	–	–	–	11.18	2.27	–	–	84.27	2.27	–
2	–	–	–	11.73	3.19	–	–	82.96	2.12	–
3	68.66	3.25	0.35	2.41	19.54	2.03	0.88	2.89	–	–
4	66.34	3.83	–	5.91	17.97	3.40	–	2.54	–	–
5	69.54	3.56	–	2.49	12.61	1.58	0.75	8.90	–	0.58
6	68.21	3.55	–	1.94	21.51	2.69	0.70	1.40	–	–
7	68.34	2.69	–	1.39	23.71	2.24	0.55	1.08	–	–

elongated, differently oriented needles. A small amount of Si probably comes from the process of sandblasting. The framework contains grains and precipitates, which is characteristic of the sintered alloy. The bonder (2–3 μm thick) with a homogeneous structure, but containing small spherical pores, is visible on the layer of the framework (Point 3). Its chemical composition is characteristic of bonding oxides, with the highest content of SiO_2, then TiO_2, K_2O, Na_2O, Al_2O_3, and less CaO. A small amount of Mg is also visible. Points 4 and 5, characteristic for the opaque layer (150 μm thick), have a crystalline structure containing: TiO_2, SiO_2, Na_2O, Al_2O_3, K_2O, CaO, and ZrO_2. Spherical pores differentiated in terms of diameter of 2-10 μm are visible in the opaque. The next adhesive layer is dentine with a homogeneous melted structure and few pores (Points 6 and 7). There are also oxides – mainly SiO_2. In addition, Na_2O, K_2O, TiO_2, and CaO are present, and Al_2O_3, but less than in the opaque.

Due to the properties of titanium, such as high affinity to oxygen, low thermal expansion, allotropic transformation of the crystal structure at the temperature of 882°C, titanium presents some problems in the process of veneering with ceramics. Titanium low thermal expansion coefficient of 10 μm/m K compared to approx. 14 μm/m K for base alloys and the transformation of the α phase during cooling below 882ºC make it impossible to use conventional ceramics to veneer titanium. These properties led to the development of ceramic masses with a firing temperature below 882ºC. Ultra-low-melting ceramics with a melting point in the range of 700–850ºC were used for veneering samples of titanium and its alloys. The preparation of titanium surfaces for bonding with ceramics consisted of jet cleaning, etching, and the use of intermediate layers. Sandblasting with Al_2O_3 with a grain size of 250 μm at a pressure of 2–3 bar was used. In the case of titanium, grains with larger diameters provide better adhesion than fine grains of 50 μm. Fine grains can be pressed into the surface, which leads to a weakening of the bond with the ceramics. After sandblasting, etching was applied to clean the veneered surface and increase roughness. Etching reduced the thickness of the oxide layer. To ensure a better contact of the titanium biomaterial with the ceramics, an intermediate layer was used – a bonder, followed by two opaque layers to eliminate the metallic colour, as well as opaque dentin. The next fired layers of ceramics are dentine and enamel.

Materials for all-ceramic restorations use a wide range of crystalline phases, which constitute the load-bearing structure. They contain up to 90% of these phases by volume. The selection of the refraction indexes of the crystalline phase and the vitreous matrix is an important factor determining endurance parameters and translucency of the ceramics. The two newest groups of all-ceramic materials for the CAD/CAM system are the following:

- Those based on lithium disilicate $Li_2Si_2O_5$, veneered with ceramics with a selected expansion coefficient, here with IPS e.max Ceram; and,
- Those based on yttria-stabilized tetragonal zirconia ZrO_2 (3Y-TZP), veneered with Elephant Sakura ceramics.

The SEM image of the microstructure of a glass-ceramic load-bearing framework veneered with low-melting point glass ceramics using the IPS e.max Ceram shows three layers (**Fig. 9** and **Tab. 6**). The basic crystalline phase, up to 60%, is lithium disilicate $Li_2Si_2O_5$. The framework consists of prismatic lithium disilicate crystals (0.5 to 5 μm long) dispersed in a glass matrix (Points 1 and 2) **[L. 2]**. Moreover, Na_2O, K_2O, Li_3PO_4, and Al_2O_3 are present in the framework. The next layer is an opaque dentin, which, in addition to the basic system, shows increased content of Na_2O, Li_3PO_4, and K_2O, and additionally F (Point 3). In dentin, the basic system and $Ca_3(PO_4)_3F$ fluoroapatite can be observed (Points 4–6).

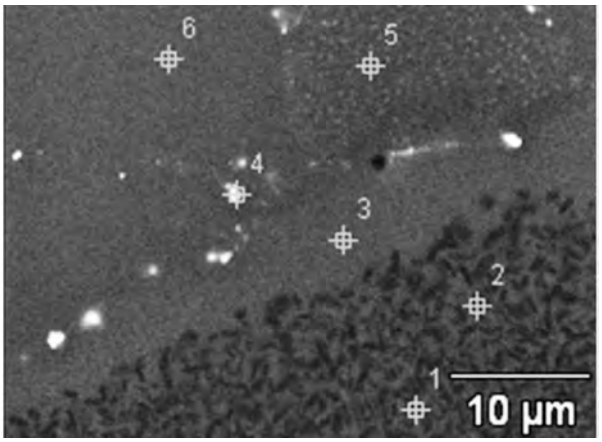

Fig. 9. The SEM image of the microstructure of the IPS e.max Ceram – $Li_2Si_2O_5$ material composition made using the milling technology with the points marked for chemical composition analysis

Rys. 9. Obraz SEM mikrostruktury kompozycji materiałowej IPS e.max Ceram – $Li_2Si_2O_5$ z technologii frezowania z zaznaczonymi punktami do analizy składu chemicznego

The SEM image of the Elephant Sakura – ZrO_2 microstructure shows a two-layer structure (**Fig. 10, Tab. 7**). The framework contains very fine uniform grains with very little pores in small quantities. The microstructure of this ceramics consists of densely packed tetragonal crystals with a particle size of 0.2–0.4 μm. The chemical analysis of Points 1 and 2 shows the presence of ZrO_2 and trace amounts of K. The K content may result from the application of chemical enhancement transformation of ZrO_2 which is based on the exchange of small alkaline ions in the glass matrix network, such as sodium ions with larger potassium ions, diffusing from molten salt baths **[L. 2].** The ion exchange by diffusion is usually carried out at

Table. 6. Chemical composition of the selected points on the specimen surface in a sample of $Li_2Si_2O_5$ made using the milling technology veneered with IPS e.max Ceram ceramics

Tabela 6. Skład chemiczny w wybranych punktach na powierzchni zgładu w próbce z $Li_2Si_2O_5$ z technologii frezowania licowanej ceramiką IPS e.max Ceram

Concentration (wt.%)								
Point	Element							
	O	F	Na	Al	Si	P	K	Ca
1	55.49	–	4.07	1.20	33.89	1.61	3.74	–
2	56.14	–	3.42	0.84	34.69	1.70	3.21	–
3	51.62	1.55	5.89	1.19	32.72	1.67	5.35	–
4	50.74	–	5.45	4.63	31.63	–	5.96	1.60
5	49.74	0.84	4.10	4.80	30.66	1.30	6.19	2.37
6	49.88	0.94	5.77	4.69	32.10	–	6.61	–
Atomic Share (%)								
Point	Element							
	O	F	Na	Al	Si	P	K	Ca
1	68.76	–	3.51	0.88	23.92	1.03	1.89	–
2	69.33	–	2.94	0.62	24.40	1.08	1.62	–
3	64.99	1.65	5.16	0.89	23.47	1.09	2.76	–
4	64.74	–	4.84	3.51	22.99	–	3.11	0.81
5	63.96	0.91	3.67	3.66	22.46	0.86	3.26	1.22
6	63.57	1.01	5.12	3.54	23.31	–	3.45	–

a temperature between 450 and 480°C, which excludes any stress relaxation and causes that the ceramic surface, is compressed; therefore, it is more resistant to crack propagation.

The ZrO_2 framework connects with the dentine with a very stable border. Large grains and big pores are visible in the dentin. The chemical analysis of points 3 and 4 shows the presence of SiO_2, K_2O, Na_2O, Al_2O_3, ZrO_2, and F.

Zirconium oxide has the advantage of being hard and very durable. It is also a light transmitting material. About 50% transparency makes that restorations look natural. The bending strength of zirconium varies between 840–1200 MPa. Thus, it exceeds endurance of other dental ceramics and allows for making prosthetic restorations in the area of the entire dental arch, especially within the lateral teeth, where the greatest occlusal forces are generated **[L. 3].**

Ceramics are widely used as veneering materials for crowns and bridges in fixed ceramic and metal restorations. The development of these techniques is the result of the appropriate selection of the expansion coefficient of ceramics and alloys and obtaining the optimal combination of these materials. The basic condition in the production of ceramic-metal restoration is that the thermal expansion coefficients of the veneering ceramics are slightly lower than that of the metal **[L. 2, 4, 5]**. As a result, during cooling, ceramics are subjected to slight compressive stresses, which provide greater resistance to cracking and chipping. When veneering with ceramics, air bubbles forming pores visible in the images of the specimens are a problem. Pores are the result of air being trapped during the sintering process. Under the influence of surface tension, air spaces become spherical and expand with increasing temperature. Under the influence of loads, they can cause crack propagation and chipping of the ceramics (**Fig. 11**). The veneering of the framework ensures that the restorations have colour stability, are biocompatible with the surrounding tissues, and chemically stable. In addition, they are characterized by a low heat transfer coefficient. Testing veneering structures allows one to modify firing of the opaque, dentin and glazing layers. The use of digital technologies, i.e. milling and SLM, for the production of load-bearing structures with CAD/CAM in prosthetics, gave rise to the need to assess the quality of veneering layers. The veneering of CoCrMo load-bearing structures is described in the works that evaluate the bond strength between the veneering ceramics and the framework **[L. 6]**, and they compare the mechanical properties and strength of such a connection **[L. 4]** and analyse the procedures for joining ceramics with CoCrMo alloy **[L. 7].**

Problems are caused by the veneering load-bearing titanium structures made using milling and SLM. This is indicated by the research and numerous literature reports in which procedures are sought for surface conditioning, optimization of the alloy composition, chemical modification of the superficial layer of the framework, and the optimization of the application and firing ceramics **[L. 8–14].**

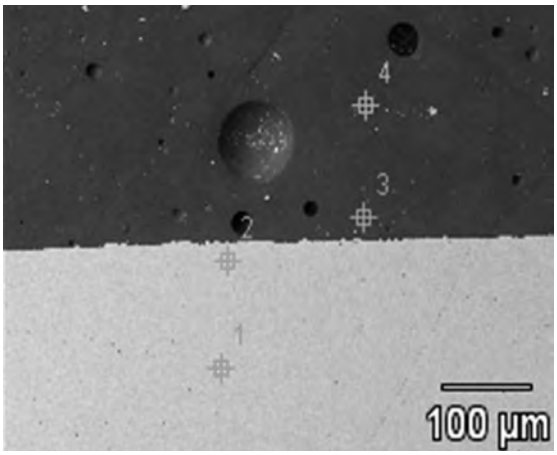

Fig. 10. The SEM image of the microstructure of Elephant Sakura – ZrO_2 material composition made using the milling technology with the points marked for chemical composition analysis

Rys. 10. Obraz SEM mikrostruktury kompozycji materiałowej Elephant Sakura – ZrO_2 z technologii frezowania z zaznaczonymi punktami do analizy składu chemicznego

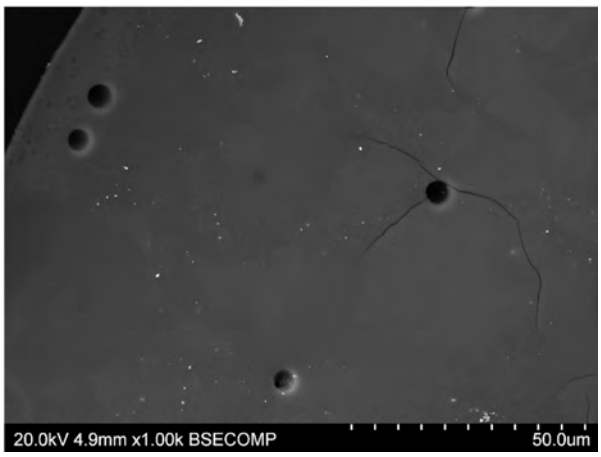

Fig. 11. The SEM image of the microstructure of the Duceram Kiss – CoCrMo material composition made using the SLM technology – crack propagation in the dentin

Rys. 11. Obraz SEM mikrostruktury kompozycji materiałowej Duceram Kiss – CoCrMo z technologii SLM – propagacja pęknięcia w dentynie

Table 7. Chemical composition of the selected points on the specimen surface in a sample of ZrO_2 made using the milling technology veneered with Elephant Sakura ceramics

Tabela 7. Skład chemiczny w wybranych punktach na powierzchni zgładu w próbce z ZrO_2 z technologii frezowania licowanej ceramiką Elephant Sakura

Concentration (wt.%)							
Point	Element						
	O	F	Na	Al	Si	K	Zr
1	29.53	–	–	–	–	0.42	70.06
2	32.10	–	–	0.20	0.86	0.36	66.47
3	50.77	–	3.86	6.65	26.97	6.82	4.93
4	51.19	1.07	6.69	4.13	28.72	5.87	2.32
Atomic (%)							
Point	Element						
	O	F	Na	Al	Si	K	Zr
1	70.33	–	–	–	–	0.41	29.27
2	72.11	–	–	0.27	1.10	0.33	26.19
3	66.43	–	3.52	5.16	20.11	3.65	1.13
4	65.32	1.15	5.94	3.13	20.87	3.07	0.52

Much research is devoted to the assessment of the veneering of the milled zirconium framework. The authors analyse the adhesion of the veneering ceramics to the zirconium framework **[L. 15–17]**, the quality of veneering with various types of modified ceramics and modified framework surfaces [**L. 18–20]**, resistance to shearing of the veneering layer **[L. 21, 22]**, and the influence of mismatch in thermal expansion coefficients on the development of residual stresses in the veneering layers **[L. 23]**.

CONCLUSIONS

The analysis of layered material compositions used in prosthetic crowns made on frameworks using digital technologies allows for praising the veneering process carried out on metal and ceramic frameworks obtained using CAD/CAM milling technology and on metal frameworks produced by SLM technology.

The research allowed us to identify the following phenomena that may be unfavourable for the process of veneering:

- The delamination of the boundary zone between the metal framework made of cobalt-chromium alloy and the opaque which may be caused by the presence of Cr_2O_2-rich oxides layer; and,
- The initiation and propagation of cracks in air bubbles, which may cause delamination of the veneering ceramics, especially when the bubbles are in the area of occlusal contact when wearing a prosthetic restoration.

Air micro-bubbles located in the deep layers of the veneering layer, with the appropriate endurance parameters of the ceramics, can act as a shock absorber for biomechanical loads in the stomatognathic system.

Microstructural and chemical analyses indicate that the material diversity of ceramic veneering layers used in metal frameworks made of CoCrMo, TiCP, and Ti6Al4V creates a number of physical, chemical, and endurance problems that can be overcome in professional veneering procedures.

The veneering of frameworks made of titanium and titanium alloy poses problems due to the need to use low-melting point ceramics in order to ensure the penetration of Ti ions into the ceramic layers. Proper preparation of the superficial layer of the framework and the correct configuration of oxides brings positive results.

The most optimal solution in terms of endurance, aesthetics, and biocompatibility is a material composition consisting of the zirconium framework stabilized with yttrium, veneered with silica ceramics.

ACKNOWLEDGEMENT

This work is financed by AGH University of Science and Technology, Faculty of Mechanical Engineering and Robotics: subvention No. 16.16.130.942.

REFERENCES

1. Ryniewicz W., Ryniewicz A.M., Bojko Ł., Leszczyńska-Madej B., Ryniewicz A.: Analysis of surface microgeometry and structure of layered biomaterials used for prosthetic constructions in digital technologies. Tribologia, 5(2019), pp. 101–113.
2. Sakaguchi R.L., Powers J.M.: Craig's restorative dental materials. Elsevier Health Sciences, Philadelphia 2012.
3. Okoński P., Lasek K., Mierzwińska-Nastalska E.: Clinical apllication of selected ceramic materials. Protetyka Stomatologiczna, 62, 3(2012), pp. 181–189.
4. Han X., Sawada T., Schille C., Schweizer E., Scheideler L., Geis-Gerstorfer J., Spintzyk S.: Comparative analysis of mechanical properties and metal-ceramic bond strength of Co-Cr dental alloy fabricated by different manufacturing processes. Materials, 11, 10(2018), p. 1801.
5. Papia E., Arnoldsson P., Baudinova A., Jimbo R., Von Steyern P.V.: Cast, milled and EBM-manufactured titanium, differences in porcelain shear bond strength. Dental materials journal, 37, 2(2018), pp. 214–221.
6. Bae E.J., Kim H.Y., Kim W.C., Kim J.H.: In vitro evaluation of the bond strength between various ceramics and cobalt-chromium alloy fabricated by selective laser sintering. The journal of advanced prosthodontics, 7, 4 (2015), pp. 312–316.
7. Antanasova M., Kocjan A., Kovač J., Žužek B., Jevnikar P.: Influence of thermo-mechanical cycling on porcelain bonding to cobalt–chromium and titanium dental alloys fabricated by casting, milling, and selective laser melting. Journal of prosthodontic research, 62, 2 (2018), pp. 184–194.
8. Fukuyama T., Hamano N., Ino S.: Effects of silica-coating on surface topography and bond strength of porcelain fused to CAD/CAM pure titanium. Dental materials journal, 35, 2 (2016), pp. 325–332.
9. Yang J., Kelly J.R., Bailey O., Fischman G.: Porcelain-titanium bonding with a newly introduced, commercially available system. The Journal of prosthetic dentistry, 116, 1 (2016), pp. 98–101.
10. Guilherme N., Wadhwani C., Zheng C., Chung K.H.: Effect of surface treatments on titanium alloy bonding to lithium disilicate glass-ceramics. The Journal of prosthetic dentistry, 116, 5 (2016), pp. 797–802.
11. Antanasova M., Jevnikar P.: Bonding of dental ceramics to titanium: processing and conditioning aspects.Current Oral Health Reports, 3, 3 (2016), pp. 234–243.

12. Sendao I.A., Alves A.C., Galo R., Toptan F., Silva F.S., Ariza E.: The effect of thermal cycling on the shear bond strength of porcelain/Ti–6Al–4V interfaces. Journal of the mechanical behavior of biomedical materials, 44 (2015), pp. 156–163.
13. Parchańska-Kowalik M., Wołowiec-Korecka E., Klimek L.: Effect of chemical surface treatment of titanium on its bond with dental ceramics. The Journal of prosthetic dentistry, 120, 3 (2018), pp. 470–475.
14. Golebiowski M., Wolowiec E., Klimek L.: Airborne-particle abrasion parameters on the quality of titanium-ceramic bonds. The Journal of prosthetic dentistry, 113, 5 (2015), pp. 453–459.
15. Qi G., Huiqiang S., Yijun H., Jia C., Weishan D.: Effect of different surface processes on the bond strength between zirconia framework and veneering ceramic. Hua xi kou qiang yi xue za zhi= Huaxi kouqiang yixue zazhi= West China journal of stomatology, 35, 6 (2017), pp. 598–602.
16. Kanat-Ertürk B., Çömlekoğlu E.M., Dündar-Çömlekoğlu M., Özcan M., Güngör M.A.: Effect of veneering methods on zirconia framework – Veneer ceramic adhesion and fracture resistance of single crowns. Journal of Prosthodontics, 24, 8 (2015), pp. 620–628.
17. Gautam C., Joyner J., Gautam A., Rao J., Vajtai R.: Zirconia based dental ceramics: structure, mechanical properties, biocompatibility and applications. Dalton Transactions, 45, 48 (2016), pp. 19194–19215.
18. Kirmali O., Kapdan A., Kustarci A., Er K.: Veneer ceramic to Y-TZP bonding: comparison of different surface treatments. Journal of Prosthodontics, 25, 4(2016), pp. 324–329.
19. Grohmann P., Bindl A., Hämmerle C., Mehl A., Sailer I.: Three-unit posterior zirconia-ceramic fixed dental prostheses (FDPs) veneered with layered and milled (CAD-on) veneering ceramics: 1-year follow-up of a randomized controlled clinical trial. Quintessence International, 46, 10 (2015), pp. 871–880.
20. Pharr S.W., Teixeira E.C., Verrett R., Piascik J.R.: Influence of Veneering Fabrication Techniques and Gas-Phase Fluorination on Bond Strength between Zirconia and Veneering Ceramics. Journal of Prosthodontics, 25, 6 (2016), pp. 478–484.
21. Zaher A.M., Hochstedler J.L., Rueggeberg F.A., Kee E.L.: Shear bond strength of zirconia-based ceramics veneered with 2 different techniques. The Journal of prosthetic dentistry, 118, 2 (2017), pp. 221–227.
22. Craciunescu E., Sinescu C., Negrutiu M.L., Pop D.M., Lauer H.C., Rominu M., Antoniac I.: Shear bond strength tests of zirconia veneering ceramics after chipping repair. Journal of adhesion science and Technology, 30, 6 (2016), pp. 666–676.
23. Mainjot A.K., Najjar A., Jakubowicz-Kohen B.D., Sadoun M.J.: Influence of thermal expansion mismatch on residual stress profile in veneering ceramic layered on zirconia: Measurement by hole-drilling. Dental Materials, 31, 9 (2015), pp. 1142–1149.